**Journal of Computing and Electronic Information Management**
ISSN: 2413-1660 | Vol. 19, No. 2, 2025

# Research on edge detection method of visual system

**Shenghu Pan, Pengcheng Zhang**

School of Mechatronics Engineering, Southwest Petroleum University, Chengdu 610500, China

**Abstract:** An edge detection algorithm based on Bertrand surface model was proposed to solve the problem of insufficient edge detection accuracy in current visual systems First of all, through the traditional detection algorithm of image contour edge contour pixel level, secondly, according to the basic principle of gradient value algorithm, combined with overall image pixel gray level distribution, calculated the whole pixel displacement and displacement based on pixel, regain Bertrand surface of subpixel edge curve, and then realize the edge detection Finally, a visual system is used to detect the edge of the measuring block, and the experimental results show that the improved Bertrand surface sub-pixel edge detection algorithm has higher accuracy.

**Keywords:** Edge detection; Bertrand surface; Gradient algorithm; Subpixel curve.

## 1. Introduction

As industrial production continues to increase, vision systems have been used in many occasions. At present, high-precision edge detection algorithms are an important way to improve the detection accuracy of the vision system. Sub-pixel edge detection algorithms can achieve high-precision edge detection while the hardware conditions of the vision system remain unchanged, and have become a research hotspot at this stage. For example, A.A.Abramenko[1] et al. used algebraic moments to obtain sub-pixel parameters of edges and increase the mask size to improve sub-pixel edge detection accuracy; Anna Fabijańska[2] et al. used a Gaussian function to reconstruct the gradient function near the thick edge and determine its sub-pixel position, thereby improving detection accuracy; Chen Liyan et al.[3] used a combination of Zermike moment algorithm and maximum entropy-like threshold method to extract the edge of the outline, and repeatedly adjusted the threshold to improve the accuracy of the image outline; Zhu Shuaifei et al.[4] used iterative method to calculate the best threshold of the step gray matrix to improve subpixel edge positioning, so as to obtain higher-precision contours; Liu Lingxiao et al.[5] proposed using the arc-tangent function model to improve subpixel edges, find target contours, and improve the success rate of contour recognition; Dai Zongxian et al.[6] proposed a recognition method that combines linear interpolation algorithm and gray curve graph, which improves the accuracy of image contours; Cui Xinnan et al.[7] proposed a moving least squares surface fitting method based on Gaussian basis functions to improve the accuracy of subpixel positioning.

These methods can be divided into three types: interpolation methods, moment methods, and fitting methods. The key to the interpolation method is to interpolate the pixels of the function image and their derivatives, so as to achieve sub-pixel. For edge detection, the advantage of interpolation method is that it is simple to calculate, but it is easily disturbed by noise; the moment method uses a series of moment models to locate sub-pixel edges. Its characteristics are similar to the interpolation method and the calculation amount is small, but this method is sensitive to noise; the principle of the fitting method is to fit the edge gray value or gradient amplitude of the image. It has strong anti-noise ability and high positioning accuracy. However, due to the complexity of the model, the calculation amount is large.

Combined with the analysis of the above methods, an algorithm based on Bertrand surface fitting is proposed. The algorithm uses a fitting method to reduce the impact of noise on the accuracy of edge contours. It uses the properties of Bertrand surfaces to reduce the calculation amount of the fitting algorithm. At the same time, the sub-pixel edge curve of the Bertrand surface is obtained again according to the gradient value algorithm, which improves the accuracy of contour recognition.

## 2. Bertrand Surface Model

If the principal normals of curve $\Gamma_1$ and curve $\Gamma_2$ coincide at corresponding points, then both curves $\Gamma_1$ and $\Gamma_2$ are referred to as generalized Bertrand curves. As shown in Figure 1 the expression for curve $\Gamma_2$ can be calculated from curve $\Gamma_1$: $\mathrm{R}_1(s)$ ,given by:

$$\mathrm{R}_2(s) = \mathrm{R}_1(s) + r(e_2 \cos\alpha + e_3 \sin\alpha) \quad (1)$$

Where $r$ and $\alpha$ denote the radial distance and polar angle, respectively, and $e_2$ and $e_3$ are the unit principal normal and unit binormal vectors, respectively.

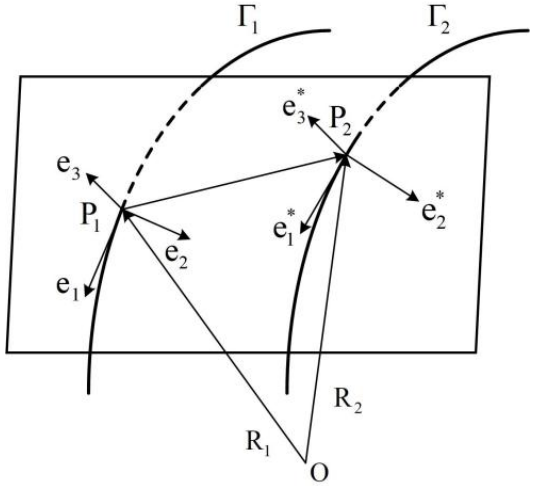


**Figure 1.** Bertrand curve

Since the radial distance and polar angle can take any numerical values, an infinite number of curves described by Equation (1) can be formed, constituting a Bertrand curve

family. By organizing two Bertrand curves according to the functional relationship $r = r(\theta)$, one obtains a generalized family of curves; the Bertrand surface is the surface formed by this family of curves [2].

As shown in Figure 2, the expression for the Bertrand surface is:

$$\mathrm{R}(s,\theta) = \mathrm{R}_{\mathrm{p}}(s) + \mathrm{R}_{\mathrm{q}}(s,\theta) \tag{2}$$

where $\mathrm{R}_{\mathrm{p}}(s)$ is the directrix of curve $\Gamma_1$, and $\mathrm{R}_{\mathrm{q}}(s,\theta)$ is a curve lying in the normal plane of the directrix, called a generatrix. The generatrix can be expressed in terms of the radial distance $\mathrm{r}$ and polar angle $\theta$; thus, the equation of the Bertrand surface is:

$$\begin{aligned} \mathrm{R}(s,\theta) &= \mathrm{R}_{\mathrm{p}} + \mathrm{r}(\theta)[e_2\cos\alpha + e_3\sin\alpha] \\ \alpha &= \alpha_1 + \theta \\ \alpha_1 &= -\int \tau(s)ds \end{aligned} \tag{3}$$

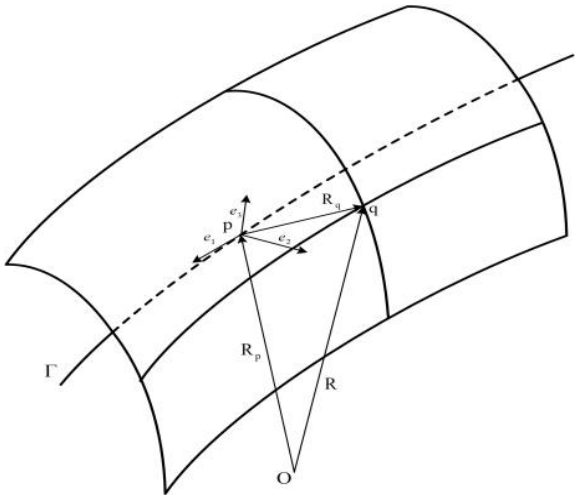


**Figure 2.** Bertrand Surface

From the above equation, it can be seen that the surface normals of the Bertrand surface at all points along a generatrix lie in the same plane as the generatrix itself [8]. Exploiting this property during Bertrand surface fitting, the pixel information from the edge contour is projected onto the normal direction of the point being estimated. In other words, multiple pixel values along the sub-pixel edge contour are aggregated within the same plane. This approach reduces the computational cost of the fitting algorithm and mitigates the impact of errors on the edge contour.

As shown in Figure 3, the edge grayscale surface can be regarded as a surface whose generatrix is the Gaussian integral curve of the Bertrand surface and whose directrix is the sub-pixel edge curve. Therefore, solving for the directrix $\mathrm{R}_{\mathrm{P}}(s)$ of the Bertrand surface yields the sub-pixel edge curve [9].

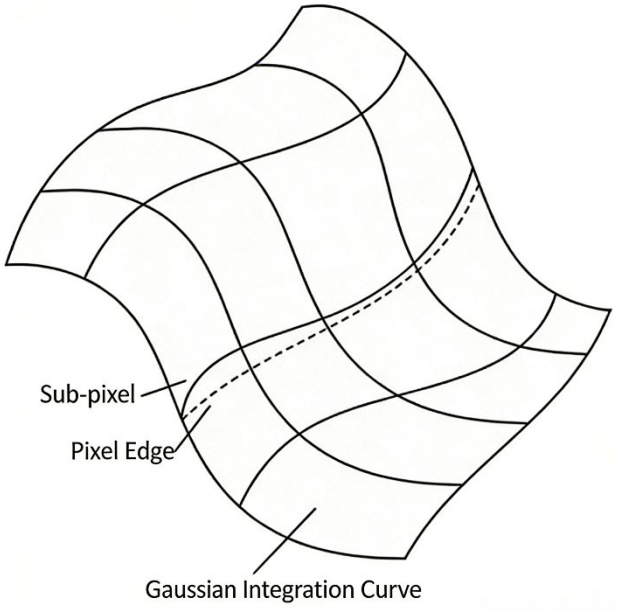


**Figure 3.** Edge grayscale surface

## 3. 8-neighbor tracking algorithm

Obtaining sub-pixel edge curves first requires the extraction of pixel-level edge curves, which can be achieved using the 8-neighbor tracking algorithm. The fundamental principle of the 8-neighbor algorithm involves locating the initial pixel of an edge. The pixels adjacent to this point are referred to as its eight neighboring pixels. Designating this pixel as the starting point C, the algorithm searches among the eight neighboring pixels in a counter-clockwise direction to identify the subsequent boundary point.

| | | |
|---|---|---|
| 3 | 2 | 1 |
| 4 | C | 0 |
| 5 | 6 | 7 |

**Figure 4.** Eight neighboring pixels

The basic steps of the 8-neighbor tracking algorithm [10]:

1) Determine the initial point of the 8-neighbor algorithm.
2) Trace and extract the pixels in the 8-neighborhood of the initial point.
3) Determine the termination criteria for the algorithm.

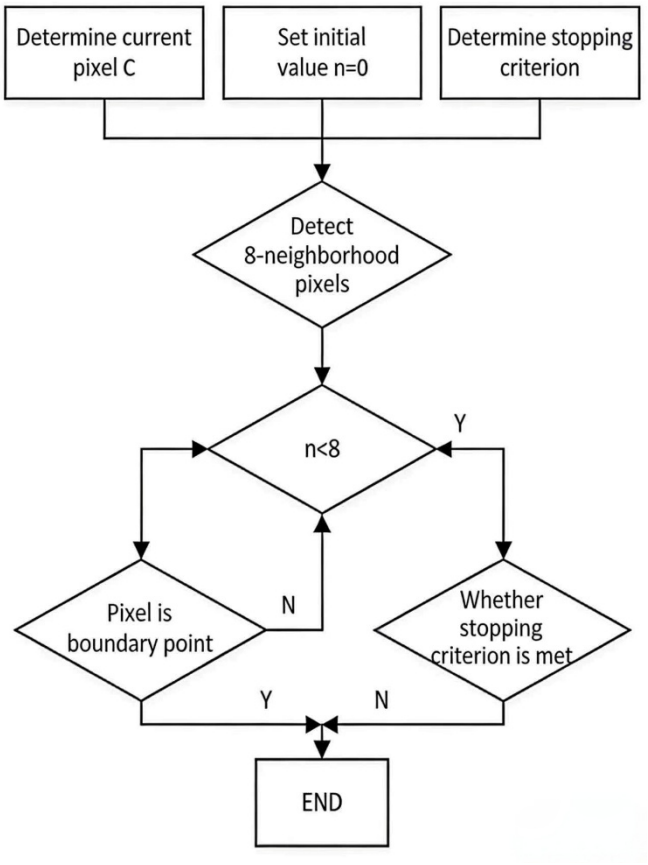


**Figure 5.** Flowchart of the eight-neighborhood algorithm

# 4. Improved Bertrand Surface Model

## 4.1. Gradient Method

To further improve the accuracy of the edge contours fitted by the Bertrand surface model, the fundamental principles of the gradient algorithm are incorporated. By calculating the sub-pixel displacement based on the integer pixel displacement, the sub-pixel edge curve of the Bertrand surface is re-established, thereby enhancing the precision of edge detection. The basic principle of the gradient algorithm is that, due to the minimal displacement during image deformation, it can be assumed that the shape remains unchanged and only the position shifts. Consequently, the grayscale value of the same point remains constant before and after the deformation [9]. That is:

$$\left.\begin{aligned} f(x,y) &= g(x',y') \\ x' &= x+\mu+\Delta x \\ y' &= y+v+\Delta y \end{aligned}\right\} \tag{4}$$

In Equation 4, $u$ and $v$ represent the pixel-level displacements of the point, respectively; $\Delta x$ and $\Delta y$ represent the corresponding sub-pixel displacements based on the pixel-level displacements, which can be calculated from $f(x,y)$ and $g(x',y')$. Then, performing a Taylor expansion on the displacement components yields the following Expansion 5.

$$\left.\begin{aligned} g(x+\mu,y+v) &= f(x-\Delta x,y-\Delta y) \\ &= f(x,y)-\frac{\partial f}{\partial x}\Delta x-\frac{\partial f}{\partial y}\Delta y \\ f(x,y) &= g(x+\mu+\Delta x,y+v+\Delta x) \\ &= g(x+\mu,y+v)+\frac{\partial g}{\partial x}\Delta x+\frac{\partial g}{\partial y}\Delta y \end{aligned}\right\} \tag{5}$$

According to the above formula, we can get:

$$(\frac{\partial f}{\partial x}+\frac{\partial g}{\partial x})\Delta x+(\frac{\partial f}{\partial x}+\frac{\partial g}{\partial x})\Delta y=2(f-g \tag{6}$$

$\mathrm{a}=\frac{\partial f}{\partial x}+\frac{\partial g}{\partial x}$ , $\mathrm{b}=\frac{\partial f}{\partial y}+\frac{\partial g}{\partial y}$ , $\mathrm{c}=2(f-g)$ , The sub-pixel displacement $\Delta x$ and $\Delta y$ can be solved by the least square method based on the whole pixel displacement.

$$\begin{bmatrix}\Delta x\\ \Delta y\end{bmatrix}=A^{-1}C \tag{7}$$

Inside, $\mathrm{A}=\begin{bmatrix}\sum a^2 & \sum ab\\ \sum ab & \sum b^2\end{bmatrix}$, $\mathrm{C}=\begin{bmatrix}\sum ac\\ \sum bc\end{bmatrix}$

## 4.2. Improved Bertrand Surface Model

The traditional Bertrand surface model assumes that the pixel edge contour and the sub-pixel edge contour of the image are relatively close. It approximates the unit tangent vector and unit normal vector of the sub-pixel edge contour using those of the pixel-level edge contour. Specifically, the equation for the sub-pixel edge curve can be obtained using the edge curve $\mathrm{R}_1(s)$ and the normal distance function $\mu(s)$ at the corresponding points of the pixel-level and sub-pixel edge curves [10]

$$\mathrm{R}_\mathrm{p}(s)=\mathrm{R}_1(s)+\mu(\mathrm{s})\mathrm{e}_2(s) \tag{8}$$

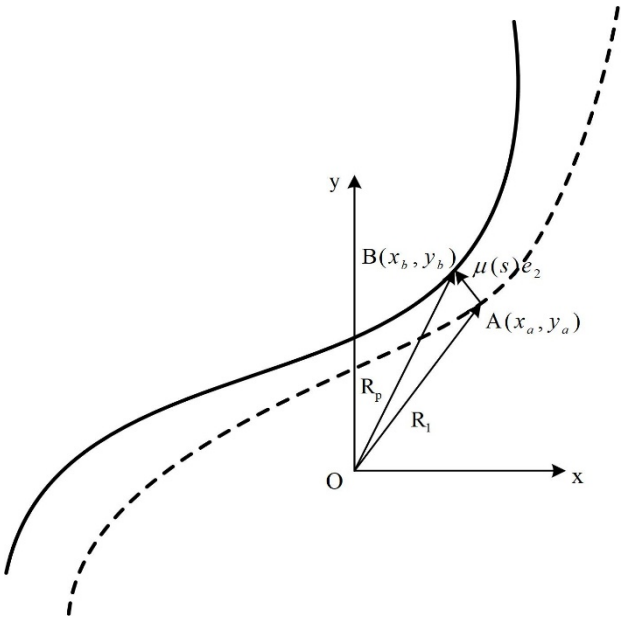


**Figure 6.** Edge Relationship

Since the sub-pixel equation is obtained by merely approximating the unit tangent and unit normal vectors, the resulting edge contour may suffer from reduced accuracy. Therefore, to minimize the error as much as possible, the

gradient method is combined to determine the vector between the pixel point and the corresponding sub-pixel point, thereby deriving the images sub -pixel edge equation.

In the same image, we can assume the pixel displacements $u$ and $v$ are zero, allowing us to recalculate the grayscale expression before and after deformation from Expansion 5 as $f(x, y) = $ $f(x,y) = g(x+\Delta x, y+\Delta y)$. As shown in the aforementioned Figure 6, the traditional Bertrand surface model approximates the sub-pixel edge curve by calculating the normal distance $\mu(s)$ between the pixel-level edge contour and the sub-pixel edge contour at corresponding points. In contrast, the Bertrand surface model combined with the gradient value method avoids the use of the unit tangent and unit normal vectors, instead calculating the sub-pixel edge curve using the vector equation between the pixel-level edge curve and the corresponding point on the sub-pixel edge curve. That is: ...

$$\begin{aligned} \mathrm{R}_{\mathrm{p}}(s) &= \mathrm{R}_1(s) + \overrightarrow{AB} = \mathrm{R}_1(s) + \begin{bmatrix} x_B - x_A \\ y_B - y_A \end{bmatrix} \\ &= \mathrm{R}_1(s) + \begin{bmatrix} \Delta x \\ \Delta y \end{bmatrix} \end{aligned} \tag{9}$$

The pixel-level edge curve of the image can be obtained using the 8-neighbor algorithm. Then, the displacements $\Delta x$, $\Delta y$ at the corresponding points of the pixel-level edge curve and the sub-pixel edge curve are calculated according to Equation 7, thereby deriving the images sub -pixel edge curve $\mathrm{R}_{\mathrm{p}}(s)$.

### 4.3. Model Solution Process

Based on the fundamental properties of the Bertrand surface, establish the functional relationship expression between the sub-pixel edge curve and the pixel-level edge curve.

Combining the overall distribution pattern of image pixel intensity, use the gradient method to find the sub-pixel displacements $\Delta x$ , $\Delta y$ based on the integer pixel displacement.

The vector between the pixel-level edge contour and the sub-pixel edge contour at corresponding points can be calculated from the pixel displacements $\Delta x$ , $\Delta y$ . The pixel-level edge curve is then calculated using the 8-neighbor tracing algorithm.

The sub-pixel edge curve is derived using the vector between the pixel-level edge contour and the sub-pixel edge contour at corresponding points, along with the pixel curve.

## 5. Experience

Gauge blocks are measuring instruments with smooth, flat surfaces. Due to their simple structure, good wear resistance, and high accuracy, gauge blocks are widely used in the manufacturing industry [11]. To verify that the improved Bertrand surface model has higher edge detection precision, the visual measurement system shown in Figure 7 is used to perform sub-pixel edge detection on the improved Bertrand surface model and the traditional Bertrand surface model from reference 10.

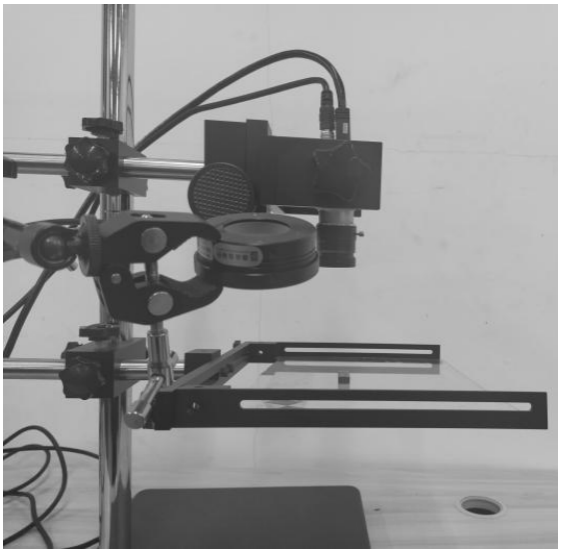

**Figure 7.** Visual Measurement System

The improved Bertrand surface model and the method from reference [10] were used to extract the local edge of a 6mm gauge block, respectively. Considering that in the Bertrand surface algorithm, a fitting region that is too large makes the calculation more cumbersome, while a region that is too small increases the precision error. To eliminate such problems as much as possible, the fitting region was set to be centered on the pixel-level edge of the gauge block, with a width of 7-9 pixels and a length equal to 5 times the transition width of the gauge blocks edge. This allows for better edge detection and ensures the fitting region meets the required fitting precision while simplifying calculations as much as possible. Based on the overall distribution pattern of image pixel intensity, the sub-pixel displacements $\Delta x$ , $\Delta y$ based on the integer pixel displacement are calculated, and the coordinates of the corresponding sub-pixel edge points are obtained. The coordinates of the corresponding sub-pixel edge points are then also obtained using the traditional Bertrand surface model algorithm from reference [10], and the edge precision detected by the different algorithms is compared.

Finally, the local edge detection of the 6mm gauge block was performed using the improved Bertrand surface model and the traditional Bertrand surface model from reference [10], as shown in Figure 8. As can be seen from Figure 8, the two different algorithms exhibit similar characteristics in detecting the edge of the gauge block. To verify the detection precision of the two algorithms, the distance from the edge points measured by the different algorithms to a straight line—using the actual edge as the benchmark—was calculated, as shown in the following Figure 9. It can be seen from this that the improved Bertrand surface model determines edge points with a smaller linearity error in the distance to the straight line compared to the traditional Bertrand surface model, which demonstrates the higher edge detection precision of the improved Bertrand surface model algorithm.

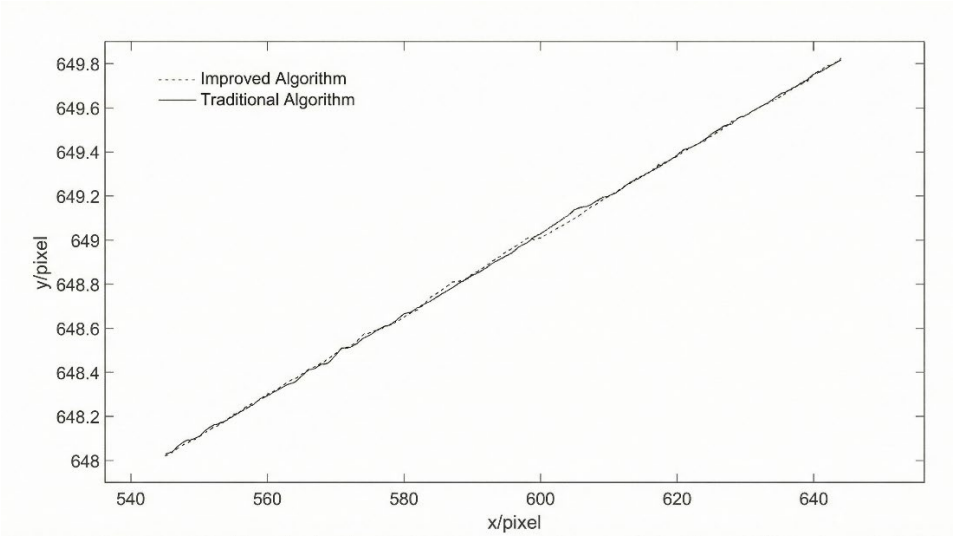


**Figure 8.** Sub-pixel Edge

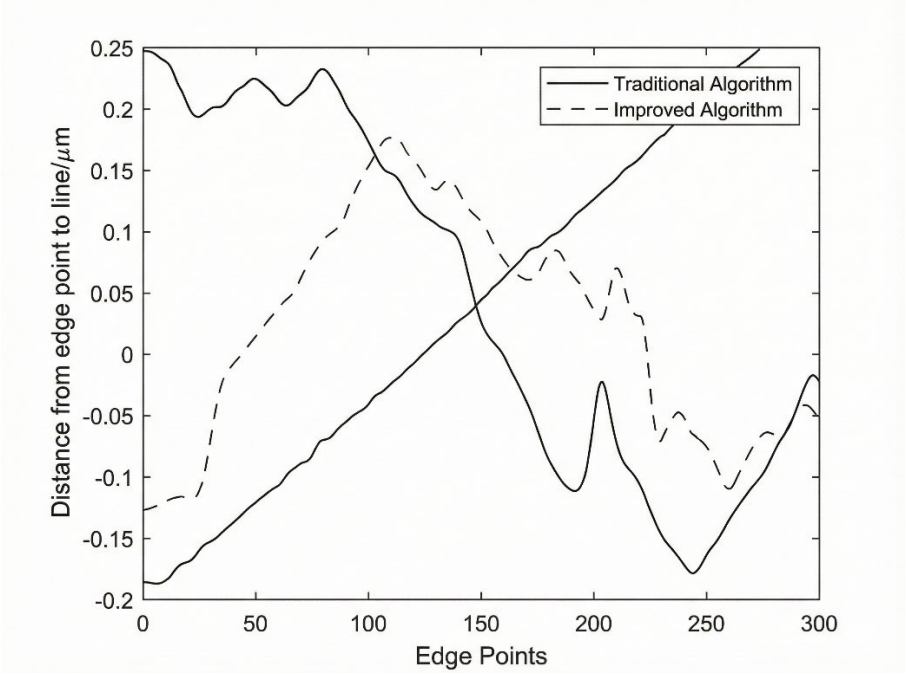


**Figure 9.** Distance from Edge Point to Straight Line

**Table 1.** Detection Results of Different Algorithms

| Measured Gauge Block | | Traditional Algorithm | | Improved Algorithm | |
|---|---|---|---|---|---|
| | | Measured Dimension(μm) | Measurement Error (μm) | Measured Dimension(μm) | Measurement Error (μm) |
| 4mm | 1 | 3999.156 | -0.844 | 4000.534 | 0.534 |
| | 2 | 4000.239 | 0.239 | 3998.526 | -1.474 |
| | 3 | 3998.354 | -1.646 | 3999.125 | -0.875 |
| | 4 | 3998.423 | -1.577 | 4000.358 | 0.358 |
| | 5 | 4000.658 | 0.658 | 3998.625 | -1.375 |
| 6mm | 1 | 5998.182 | -1.818 | 6000.256 | 0.256 |
| | 2 | 5999.068 | -0.932 | 6000.324 | 0.324 |
| | 3 | 5998.558 | -1.442 | 5998.243 | -1.757 |
| | 4 | 6001.154 | 1.154 | 5999.379 | -0.621 |
| | 5 | 5998.285 | -1.715 | 5998.537 | -1.563 |
| 8mm | 1 | 8000.256 | 0.256 | 7999.132 | -0.868 |
| | 2 | 7998.458 | -1.542 | 8000.334 | 0.334 |
| | 3 | 7999.051 | -0.949 | 7999.358 | -0.642 |
| | 4 | 8000.523 | 0.523 | 7998.893 | -1.107 |
| | 5 | 7998.422 | -1.578 | 8000.727 | 0.727 |
| Average Dimension(μm) | | -0.748 | | -0.517 | |

To better compare the edge detection precision of the improved Bertrand surface model algorithm with the

traditional Bertrand surface model algorithm, five images of the edges of 4mm、6mm、8mm gauge blocks were collected separately under constant experimental conditions. Both algorithms were used for edge detection, and the distance from one detected edge to the other (used as the benchmark) was calculated. The results are shown in Table 1.

From Table 1, it is evident that the average value of the measurement precision error for the improved Bertrand surface model is-0.517μm; whereas the average value of the measurement precision error for the traditional Bertrand surface model is -0.748μm. Therefore, it can be concluded that the edge contour detected by the improved Bertrand surface model algorithm has higher precision.

# 6. Summary

Based on the edge detection algorithm of the Bertrand surface model, this paper utilizes the global distribution patterns of image grayscale and incorporates the gradient value method to re-establish the relationship between the pixel curves and sub-pixel curves of the model. This approach allows for the accurate determination of sub-pixel edge positions in an image. Compared with the traditional Bertrand surface model algorithm, the improved algorithm significantly enhances edge detection precision. Experimental results demonstrate that the improved algorithm yields a smaller error in the distance from determined edge points to the fitted line, as well as a lower average edge detection error. Consequently, the improved Bertrand surface model algorithm offers higher accuracy and is better suited for application in visual processing systems.

# References


[1] A.A.Abramenko,A.N.Karkishchenko. Applications of algebraic moments for edge detection for locally linear model[J]. Pattern Recognition and Image Analysis,2017,27(3):

[2] Anna Fabijańska. A survey of subpixel edge detection methods for images of heat-emitting metal specimens[J]. International Journal of Applied Mathematics and Computer Science,2012,22(3):

[3] Chen L Y, Xiong Q Q. High precision adaptive detection of sub-pixel edge of optical image [J]. Laser journal,2020,41(11):86-90.(in Chinese)

[4] Zhu S F, Ma W, Yang F. Improved High-precision Localization Algorithm of Moving Target based on Zernike Moment [J]. Machinery Design & Manufacture,2021(08):235-239+245.(in Chinese)

[5] Liu L X, Wang D C, Cheng P, LANG N. Optical Technique, 201,47(05):587-593.(in Chinese)

[6] Dai Z X, MO H B, ZHOU Y, Zhang Z, Yin A J, Liang Z X. Subpixel interpolation vision measurement method based on gray scale [J]. China measurement & testing,2019,45(05):33-37.(in Chinese)

[7] Cui X N, Wang X G. Application research of computers,2020,37(S2):330-332. (in Chinese)

[8] Liu J, Chen H J, Duan Z Y, Wu H J. Research on The Basic Principle of Bertrand Conjugate Surface [J]. Journal of Dalian University of Technology,2006(02):212-219.(in Chinese)

[9] Hu J S, KANG J R, Zhang Qi, Liu P C, Zhu M D. An improved algorithm for eight-neighborhood image boundary tracking [J]. Bulletin of Surveying and Mapping,2018(12):21-25.(in Chinese)

[10] Wang N, Duan Z Y, Zhao W H, Du P, Duan Bo-qiang, Zhao Jun-gui. Edge detection algorithm based on Bertrand surface model [J]. Acta photonica sinica,2017,46(10):179-186.(in Chinese)

[11] Ning G Q. Fundamentals of Mechanical Manufacturing Quality Control Technology: Beijing University of Aeronautics and Astronautics Press,2007.(in Chinese)